NANO LETTERS

2008
Vol. 8, No. 8
2144-2149

# Theory and Application of Chain Formation in Break Junctions

**A. Thiess,† Y. Mokrousov,*,† S. Blügel,‡ and S. Heinze†**

*Institute of Applied Physics, University of Hamburg, 20355 Hamburg, Germany, and Institut für Festkörperforschung, Forschungszentrum Jülich, D-52425 Jülich, Germany*

*Received January 9, 2008; Revised Manuscript Received May 27, 2008*

## ABSTRACT

**We introduce a generic model of chain formation in break junctions by formulating criteria for the stability and producibility of suspended monatomic chains based on total energy arguments. Using *ab initio* calculations including spin-polarization and spin−orbit coupling, we apply our model to the formation of monatomic 4d and 5d transition metal (TM) chains. We explain the physical origin of the experimentally observed general trend of increasing probability for the creation of long chains for late 5d TMs and suppressed chain formation for 4d TMs. We also clarify why the probability of chain elongation can be greatly enhanced by the presence of adsorbates in experiments.**

Within the coming decade, the downscaling of conventional electronic devices will reach its limit. With the ulterior motive of realizing novel device concepts,[1,2] quantum transport in nano- or even atomic-scale structures is currently intensively explored.[3] A very promising experimental approach to study the transport properties of such nanosystems is break junction (BJ) experiments[4–10] which offer the unique possibility to explore numerous quantum phenomena and crossovers between different regimes by changing nanosized contacts in real time.

In a typical BJ experiment, the metallic leads, being initially in contact, are pulled apart and the conductance of the system is measured simultaneously. Upon pulling, atoms are extracted from the leads and may form a chain consisting of a few atoms. Up to now, successful chain formation in BJ experiments was reported for several transition metals (TMs).[6,7] While for later TM elements of the periodic table, in particular, Au and Pt, chains with quite a large number of atoms can form,[8,9] for earlier 5d and 4d metals long chain creation in BJs does not occur.[6] It was suggested that this trend is closely related to the fact that late 5d elements reveal reconstructions of the low-index surfaces and they are more strongly influenced by relativistic effects on the electronic structure.[6] Recently, it was reported that the probability of chain creation can be significantly increased by the presence of oxygen during experiments.[7,10]

Computationally, treating the complicated process of chain formation in a BJ with the accuracy of *ab initio* methods is an extremely challenging task even for the fastest schemes, since the motion of hundreds of atoms has to be taken into account on a phonon time scale.[11,12] Moreover, the exact structure of the leads is normally unknown, which leaves a great deal of uncertainty in the initial configuration of the system.[13,14] This motivates the development of generic models able to provide an insight in terms of a chemical trend. Here, we introduce a model for the chain formation in a BJ, which is based on total energy arguments leading to criteria for the stability and producibility of suspended chains. Our model can be used for predicting successful chain formation in a vast variety of BJs, including electronic effects such as spin-polarization, spin−orbit coupling and correlations. Being computationally easily accessible, it relies only on a few system specific quantities with transparent physical meaning, which helps to shed light onto the complicated process of chain formation.

Evaluating this model on the basis of density functional theory, we apply it to chain formation in BJs of 4d and 5d transition metals and reveal the key physics behind it. We predict an increased probability of creating chains at the end of the 5d series, reaching a maximum for Ir, Pt, and Au. For 4d elements, we demonstrate that the probability of chain creation is strongly reduced because of smaller relativistic effects in the electronic structure of these chains.[6] We show that small suspended chains exhibit large variations in the interatomic distance upon elongation[4] and, consequently, in their electronic and transport properties. Our model also allows for the understanding of the significantly enhanced probability of chain formation in the presence of oxygen as observed in experiments.[7]

We divide the system into two distinct regions: the leads and the suspended chain. The electronic structure of these two parts is considered separately, neglecting their mutual influence. This is a very good approximation for describing

* Corresponding author. E-mail: ymokrous@physnet.uni-hamburg.de.
† University of Hamburg.
‡ Forschungszentrum Jülich.

10.1021/nl0800671 CCC: $40.75 
**Published on Web 07/18/2008**

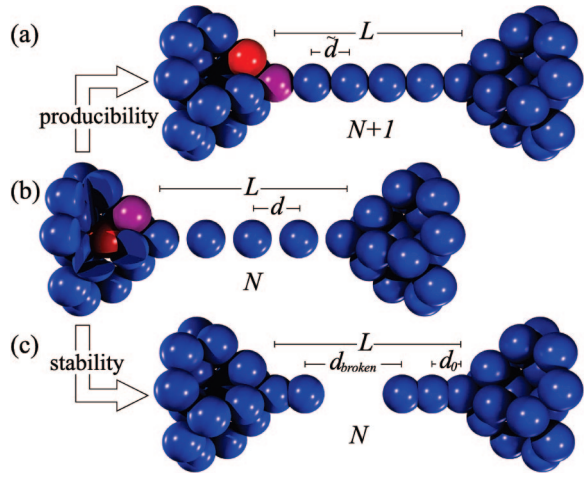


**Figure 1.** Suspended three-atoms chain ($N = 3$) under tension (b) reduces it via pulling one more atom out of the leads (a) or by breaking (c). For details see text.

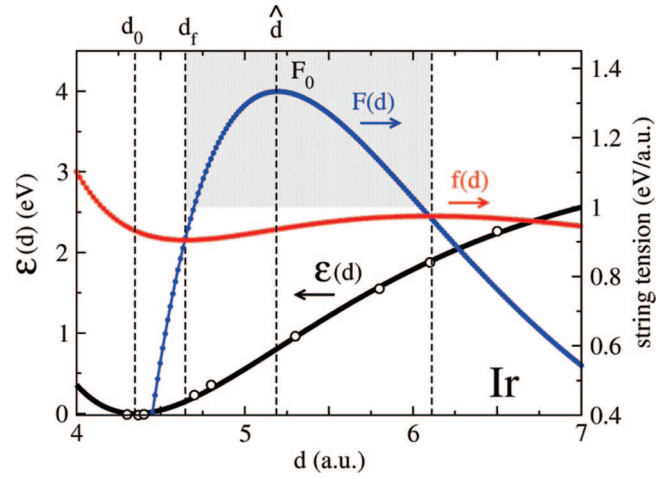


**Figure 2.** Binding energy $\mathcal{E}(d)$ relative to the MW cohesive energy $E_{MW}(d_0)$ (full line stands for the Morse potential fit of *ab initio* values indicated by open circles), as well as string tension $F(d)$ and generalized string tension $f(d)$ for an infinite Ir MW. $d_0$ marks the equlibrium interatomic distance, while $\hat{d}$ stands for the inflection point. The local minimum of the $f(d)$ is reached at $d_f$. Grey shaded area marks the region of $d$ where eq 4 is satisfied and the chain can successfully grow.

the formation of longer chains (longer than three atoms), which is the main goal of this communication. The process of chain formation is investigated by evaluating the change in total energy of an atom which alters its position from the lead into the chain. The process of increasing the number of atoms in the suspended chain is described in the so-called rapid reformation approximation (RRA). In this approximation, one assumes that only the interatomic distance in the chain is changed upon pulling the leads apart at a given number of chain atoms, while the structure of the leads remains fixed.[11,12,15] Moreover, we suppose that the transfer of a lead atom into the chain happens instantaneously at a certain time $t_0$,[10] when the energy of the transferred atom and its coordinates change suddenly from their values inside the lead to the corresponding values inside the chain. The probability for such an event, which depends on a number of characteristic material parameters, allows us to predict general trends of chain formation. In this model, kinetic processes that determine how often chain formation is observed are not considered.

The sketch of our system is presented in Figure 1. We compare the total energies of configurations (b) and (a) of Figure 1, which are the initial and final configurations, respectively, in the process of pulling one lead atom into the chain within the RRA, where $L$ is the distance between the leads. A successful chain elongation translates into the following total energy relation, the criterion for producibility (P criterion):

$$(N+1)\mathcal{E}(d) \geq \Delta E_{lead} + (N+2)\mathcal{E}(\tilde{d}) \qquad (1)$$

where $d = L/(N+1)$ and $\tilde{d} = L/(N+2)$ are the chain interatomic distances before and after elongation, respectively, and $N+1$ is the number of bonds in a chain of $N$ atoms. From the binding energy of a single atom in an infinite monowire (MW), $E_{MW}(d) = E_{MW}(d_0) + \mathcal{E}(d)$, we define $\mathcal{E}(d)$ as the binding energy of this atom relative to the MW cohesive energy at equilibrium interatomic distance, $E_{MW}(d_0)$, which implies $\mathcal{E}(d) > 0$. The chain formation energy is given by $\Delta E_{lead} = E_{MW}(d_0) - E_{lead}$, where $E_{lead}$ denotes the cohesive energy of the lead atom. At finite temperatures, $\Delta E_{lead}$ corresponds to the difference between the chemical potentials of the lead and those of the infinite wire. Typically, $\Delta E_{lead} > 0$. If criterion (1) is satisfied, configuration (a) in Figure 1 is energetically more favorable than configuration (b), and the system tends to increase the number of atoms in the chain by one.

Upon stretching, in between two elongation events, the chain has to remain stable and should not break. To analyze the stability of suspended chains, we consider the most likely way of chain rupture due to phonon excitations with subsequent instant relaxation of the two halves of the chain to the equilibrium configuration. We compare the total energies of configurations (b) and (c) of Figure 1 and assume that the chain will remain in configuration (b) with a given number of atoms $N$ and interatomic distance $d$ as long as the following criterion for stability (S criterion) holds:

$$NE_{MW}(d_0) + E_{MW}(d_{broken}) \geq (N+1)E_{MW}(d) \qquad (2)$$

where $d_{broken} = (N+1)d - Nd_0$ is the length of a broken bond, obtained within the RRA by keeping the length of the suspended chain $L$ constant during rupture. Equation 2 can be easily cast into the condition:

$$\mathcal{E}(d_{broken}) \geq (N+1)\mathcal{E}(d) \qquad (3)$$

which correctly describes the trend of decreasing stability of suspended chains with increasing number of atoms $N$ as well as the decrease of sustainable intrachain distance $d$ down to the equlibrium one $d_0$.

To apply the S and P criteria to suspended monatomic chains, it is useful to fit the MW binding energy $\mathcal{E}(d)$, calculated from *ab initio*, by a Morse potential $\mathcal{E}(d) = |E_{MW}(d_0)|\cdot(1 - e^{-\gamma(d-d_0)})^2$. Such fits are very accurate as shown for Ir in Figure 2. The cohesive energy of a chain atom $E_{MW}(d_0)$ and the elastic modulus $\gamma$ obtained from this fit can be mapped to two physically more transparent quantities, the inflection point $\hat{d} = d_0 + \ln 2/\gamma$ and the break force or

maximally sustainable string tension, $F_0 = F(\hat{d}) = \gamma E_{MW}(d_0)/2$. The string tension $F(d) = \partial\mathcal{E}(d)/\partial d = \mathcal{E}'(d)$ is displayed in Figure 2. The inflection point $\hat{d}$ gives an estimate of how far an ideal infinite chain can be stretched until it breaks by the maximum break force due to long-wavelength perturbations.[16]

From eq 1, one can conclude, that the two main parameters which compete and which determine whether a chain can be extended by one atom are the energy cost of bringing an atom from the lead into the chain, $\Delta E_{lead}$, and the break force $F_0$, which is given by the steepness of the MW binding energy curve. Physically, the reason behind a successful chain elongation event is the following: as the chain is stretched, the energy of the system increases up to the point, where a lead atom overcomes the chain formation barrier, $\Delta E_{lead}$, and enters the chain. This reduces the distance in the chain from $d$ to $\tilde{d}$ and lowers the total energy of an atom in the MW, $E_{MW}(\tilde{d}) < E_{MW}(d)$. The larger the slope of the total energy $E_{MW}(d)$, the more energy can be gained by relaxing the chain from a distance $d$ to $\tilde{d}$. Therefore, large values of $F_0$ and small energy barriers $\Delta E_{lead}$ will favor chain elongation.

In the limit of a very large number of atoms in the chain $N$, the binding energy difference, $\mathcal{E}(d) - \mathcal{E}(\tilde{d})$, can be replaced by the product of the string tension $F(d)$ and the elongation $\Delta d = d - \tilde{d} \approx L/N^2$ of the chain, $\mathcal{E}'(d)\cdot\Delta d$, and the P criterion (eq 1) can be rewritten in the following way:

$$F(d) \geq \frac{\Delta E_{lead} + \mathcal{E}(d)}{d} = f(d) \qquad (4)$$

where $f(d)$ is the generalized string tension, or the work done in drawing the chain with interatomic distance $d$ out of the leads per unit chain length. Analysis of long and thick suspended chiral gold nanowires[17] in terms of the minimum of the generalized string tension $f$ was successfully performed in the past.[18] Generally speaking, eq 4 provides an interval of $d$, in which the suspended chain can successfully grow (Figure 2). By simple differentiation of $f(d)$, it is easy to demonstrate that the lower and upper boundaries of this interval, where eq 4 becomes an equality, correspond to the local minimum and maximum of $f(d)$, respectively (see Figure 2).

Upon stretching with increasing $d$, the string tension $F(d)$ increases and the generalized string tension $f(d)$ decreases until eq 4 becomes an equality at $d = d_f > d_0$ and $f(d)$ reaches its minimum. Ideally, as soon as $d_f$ is reached, one lead atom enters the chain and the interatomic distance relaxes from $d_f$ to $\tilde{d} \approx d_f - L/N^2$, reducing the string tension, and the process repeats. In the limit of $N \rightarrow \infty$, the difference $d_f - \tilde{d}$ tends to zero and during the successful chain elongation the interatomic distance in the chain will stay at the constant value of $d_f$, which minimizes the generalized string tension. In this respect, $d_f$ serves as a quasi-equilibrium interatomic bond length of a chain under tension. However, the chain is unstable at $d_f$ according to eq 3, which states that with $N \rightarrow \infty$ the chain will not break only if $d = d_0 < d_f$. Therefore, for an adequate description of the process of chain formation in BJs, the inclusion of the fact that the chain is finite via eq 1 and eq 3 is crucial.

As a first application of our model, we investigated BJs of 4d and 5d TMs for which numerous experimental studies exist.[6,7,9,10] The 4d and 5d TM MWs are strongly magnetic in a wide range of interatomic distances,[19] revealing a large magneto-elastic effect[20] with strong influence of spin−orbit coupling (SOC) on magnetic and electronic properties.[21] The results are evaluated for the true magnetic ground state with respect to the easy axis of magnetization. The *ab initio* calculations were carried out in the generalized gradient approximation (GGA) to the density functional theory, employing the full-potential linearized augmented plane-wave method for one-dimensional (1D) systems,[22] as implemented in the FLEUR code.[23] For calculations of the bare monowires, we included basis functions with plane waves up to $k_{max} = 4.4$ a.u.$^{-1}$ and used 64 $k$-points in one-half of the 1D Brillouin zone. SOC was included self-consistently in a nonperturbative manner.[24] For spin-polarized calculations, we considered collinear ferro- and antiferromagnetic spin ordering in the chains.

We assume that, in the process of chain formation, an atom at the surface of the lead is transferred into the chain; that is, we choose as chain formation energy $\Delta E_{lead}$ the energy difference $\Delta E_{surf}$ between an atom at a low-index surface of the lead and a MW at $d_0$.[25] This is later compared with the second assumption for $\Delta E_{lead}$, where the atom is transferred directly from the bulk into the wire, calculated with the bulk version of the FLEUR code (see Figure 4a).[26]

We apply the S and P criteria given by eq 1 and eq 3 to BJs of 4d and 5d TMs and present the results explicitly in Figure 3a−f for W, Re, Os, Ir, Pt, and Au BJs in terms of ($N$, $d$) phase diagrams. In these plots, gray shaded areas indicate regions of stability (S, dark gray) or producibility (P, light gray), where the S or P criterion is satisfied, respectively. The boundary of the S region is an intrinsic chain property and marked with a solid black line. The P region depends on the crystal structure and surface orientation assumed for the leads, and its boundary is marked by a broken line with a color corresponding to the chosen lead type indicated by the legend. When the two regions are strictly separated (white areas), as for W, Re and Os, chain formation does not take place and the width of the gap is a measure of how improbable chain elongation is. Ideally, chain elongation occurs if both regions overlap (SP region, shown in green).

The results for 5d TMs, presented in Figure 3, reveal a clear trend of decreasing distance between the S and P regions in the ($N$, $d$) space with increasing d band filling. While for Hf, Ta (not shown), and W, the S and P regions are far apart, the gap starts to close for Re and Os, and for Ir, Pt, and Au these regions overlap, with the largest overlap for Au. In terms of our model, this means that a successful creation of long chains in a BJ is possible for the latter elements. This trend agrees with the experimental observation of long chains for Ir, Pt, and Au, while experiments on W result only in one to two atom chains.[27] In general, such small chains can be produced in any break junction via a thinning process during pulling the electrodes from each other, a process not considered here.[29,28] Therefore, there will always

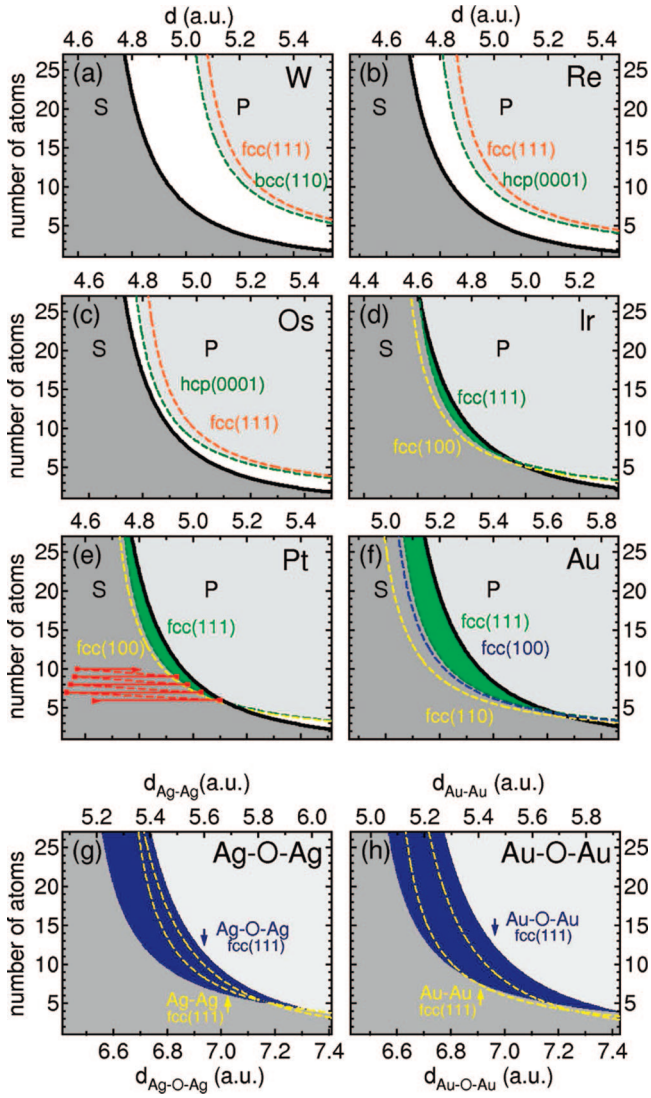


**Figure 3.** (a−f): $(N, d)$ phase diagrams for 5d TM BJs from W to Au. Plots indicate regions of stability (S, dark gray), producibility (P, light gray), separated by a white region for a−c or overlapping in the SP region for d−f. In d−f, the SP region exists for all surfaces, and the smallest of them is marked in green. The starting point along the $x$ axis is the equilibrium interatomic distance $d_0$. In e, red lines denote a typical trajectory of a suspended chain $(N(L), d(L))$ as a function of the separation between the leads $L$. (g,h) S, P, and SP regions (blue) for oxygen-assisted chain formation in BJs of Ag and Au neglecting SOC. Dashed yellow lines indicate the boundaries of the SP regions without oxygen. For further explanations see text.

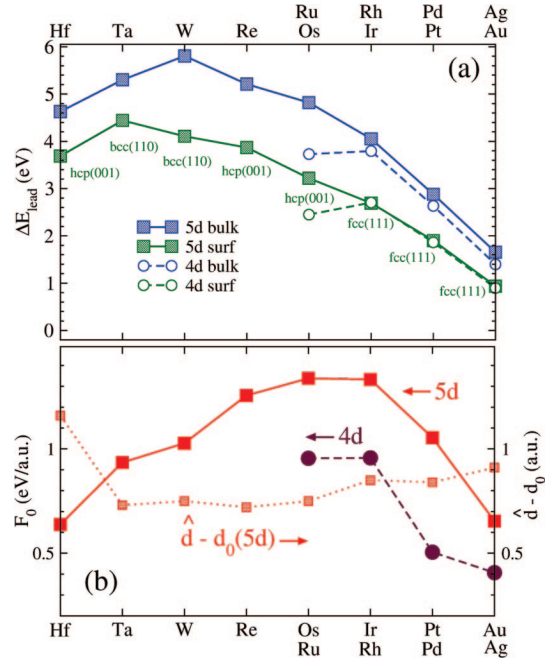


**Figure 4.** (a) Chain formation energy $\Delta E_{lead}$, defined as an energy difference between an atom in the bulk of the lead ($\Delta E_{bulk}$) or on the surface of the lead ($\Delta E_{surf}$) and an atom in the MW at $d_0$, for the 4d and 5d TMs. (b) Break force $F_0$ for the 4d and 5d TMs, and $\hat{d}-d_0$ difference for 5d TMs.

be an initial seed of a short chain which allows for growing longer chains upon further stretching, as in the case of Ir, Pt, and Au, although the SP overlap region does not exist for very small chains in this model.

With increasing number of atoms $N$, the boundaries of the S and P regions in the $(N, d)$ maps converge to the interatomic distances $d_0$ and $d_f$, $d_f > d_0$, respectively, and for large $N$, the S and P regions do not overlap. The SP regions are largest for chains with a comparatively small number of atoms, while the distances $d$ for which chain creation will occur are much larger than those estimated in the limit of large $N$ (Figure 3). For Au chains, the range of predicted interatomic distances of 5.1−5.7 a.u. is in good agreement with experiments.[8,30] Similar values have also been obtained for suspended Au chains by extensive molecular dynamics simulations including realistic leads.[15] During the process of chain elongation, described by an $(N(L), d(L))$ trajectory in $(N, d)$ space (Figure 3e) as a function of the separation between the leads $L$, large variations in $d$ will result in significant changes in chains electronic, magnetic, and transport properties,[19,31] which can be naturally accounted for in our model.

The reason for the observed trend for 5d TMs can be easily explained in our model, making use of the following observations. The maximum of the chain formation energy $\Delta E_{lead}$ is found for Ta and W (Figure 4a), chemical elements at the center of the transition metal series, while the peak in the break force $F_0$ is shifted to later elements (Figure 4b). This leads to larger values of $F_0$ and smaller values of $\Delta E_{lead}$ for late 5d TMs which, according to eq 1, results in higher probability of chain creation for these elements. Accordingly, with increasing d band filling, the P regions move closer to $d_0$. Surprisingly, the S region remains almost unchanged with respect to the band filling, being basically universal for all 5d TMs. The position of the S region with respect to $d_0$ depends only on the elastic modulus $\gamma$ of the chain or on the inflection point, respectively, which is nearly a constant for all 5d metals (see Figure 4b). For Au, the competition of small $F_0$ and $\Delta E_{lead}$ values results in the largest SP region among all 5d metals.

A variation of the crystal structure or surface orientation of the leads does not change the results crucially (c.f. Figure 3). However, lead atoms in more open surfaces, that is, with less nearest neighbors (e.g., fcc(100) vs fcc(111)), have smaller values of $\Delta E_{lead}$, which results in larger SP regions,

an effect which can be even more dramatic in a realistic situation because of a further reduced coordination of atoms at the contact of a lead, as compared with a surface. Artificially increasing the coordination number of a lead atom by taking the larger bulk energies as reference for $\Delta E_{\text{lead}}$ (Figure 4a) preserves the general trend of the S and P regions; however, they move farther apart, resulting in the absence of an overlap region for Pt, Ir, and even Au. This observation clarifies the importance of the local atomic structure of the leads for a successful chain formation and can explain the stochastic nature of chain formation observed experimentally.

The significantly diminished probability for chain creation observed experimentally for 4d TM BJs can be explained by a reduction in the values of the break force $F_0$ (Figure 4b), while the energy cost of extracting an atom from the lead, $\Delta E_{\text{lead}}$, is roughly the same as for the 5d elements (Figure 4a). In accordance with these values, we do not find an overlap region for Rh and Pd, while a small overlap exists for Ru (not shown). For Ag (Figure 4g), an SP region exists in GGA but, as opposed to Au, disappears in the local density approximation (LDA) of the exchange-correlation potential.[32]

Comparing the electronic structure of Ir, Pt, and Au chains to their 4d counterparts, Rh, Pd, and Ag, we observe that because of a relativistic mass enhancement for the heavier 5d TMs the kinetic mass of electrons in the 6s orbital increases. Consequently, the 6s orbital becomes more localized, the binding energy of the 6s electrons moves to lower energy into the region of the 5d states, which causes a stronger sd hybridization and d−d interaction along the chain axis increases. As a result, for 5d elements, the equilibrium interatomic distance $d_0$ becomes smaller, the d bandwidth becomes larger, and the bonding becomes stronger than for 4d chains, an effect also observed in small clusters.[33] This leads to larger cohesive energies for the 5d TM MWs and corresponding values of the break force $F_0$, as compared with the 4d elements, making the chain formation among the 5d chains much more likely.

The study of BJ formation in terms of S and P regions can be extended to more complex systems. In Figure 3g-h, we present the analysis of the oxygen-assisted long chain formation in BJs of Ag and Au. For simplicity, we assume that the presence of oxygen atoms in experiments results in a linear Ag−O−Ag−O−.. (Au−O−Au−O−..) chain structure in between the Ag (Au) leads. Interestingly, the modification of the binding energy curve due to oxygen leads to larger S and P regions and, correspondingly, a larger SP region, indicating a more probable chain formation as observed experimentally.[7,10] A strong hybridization of metal sd orbitals with $p_z$ orbitals of oxygen along the chain axis results in strong bonding with much larger values of $F_0$. For example, for Ag BJs, the O alternation results in an increase of the break force $F_0$ by a factor of 6. In case of Au chains doped with O, the range of predicted observable interatomic distances of 6.6 − 7.3 a.u. are in good agreement to existing experiments in which the chain creation is believed to be accompanied with light atoms in between Au bonds.[4,30,8]

Concluding, we introduce a generic model stating conditions required for successful formation of long chains in break junctions. This model allows a transparent analysis of chemical trends for a large number of systems in a short time on the basis of a few element specific parameters, which can be easily obtained by the density functional theory calculations. We found a universal trend for the stability and understand the increased producibility of suspended 5d metal chains. The prediction of long suspended chains in break junctions of Ir, Pt, and Au among the 5d metals is consistent with existing experiments and gives credibility to our model. Among the 4d metals, we predict the formation of long chains for Ru. We motivate experimentalists to take this system under scrutiny.

Despite the fact that our model is based on a number of simplifications and it most appropriately describes the elongation process in longer suspended chains, it captures the key physics of chain formation and can be used to find general trends in creating small chains in BJs. Moreover, it can be improved in a straightforward manner by including the elastic properties of the leads or considering deviations from the linear arrangements of the chain atoms to zigzag or dimer configurations. Although these nonideal atomic arrangements are most probably not essential for the properties of the chains under significant strain,[34] in some systems, they could improve the values of the total energies used for criteria for producibility, and, especially, stability,[16,35,36] as well as bring important modifications with respect to the true magnetic ground state of the wires.[20,37] Our model also allows investigating the effect of strong correlations on the producibility of chains in BJs, for example, in the spirit of LDA + $U$.

**Acknowledgment.** Financial support of the Stifterverband für die Deutsche Wissenschaft and the Interdisciplinary Nanoscience Center Hamburg are gratefully acknowledged. We would like to thank Paolo Ferriani for many fruitful suggestions at the final stage of this paper and Ruben Weht for stimulating discussions.

## References

(1) Rocha, A. R.; García-Suárez, V. M.; Bailey, S. W.; Lambert, C. J.; Ferrer, J.; Sanvito, S. *Nat. Mater.* **2005**, *4*, 335.
(2) Chappert, C.; Fert, A.; Van Dau, F. N. *Nat. Mater.* **2007**, *6*, 813.
(3) Sokolov, A.; Zhang, C.; Tsymbal, E. Y.; Redepenning, J.; Doudin, B. *Nat. Nanotechnol.* **2007**, *2*, 171.
(4) Yanson, A. I.; Rubio-Bollinger, G.; van den Brom, H. E.; Agraït, N.; van Ruitenbeek, J. M. *Nature* **1998**, *395*, 783.
(5) Ohnishi, H.; Kondo, Y.; Takayanagi, K. *Nature* **1998**, *395*, 780.
(6) Smit, R. H. M.; Untiedt, C.; Yanson, A. I.; van Ruitenbeek, J. M. *Phys. Rev. Lett.* **2001**, *87*, 266102.
(7) Thijssen, W. H. A.; Marjenburgh, D.; Bremmer, R. H.; van Ruitenbeek, J. M. *Phys. Rev. Lett.* **2006**, *96*, 026806.
(8) Kizuka, T. *Phys. Rev. B* **2008**, *77*, 155401.
(9) Untiedt, C.; Yanson, A. I.; Grande, R.; Rubio-Bollinger, G.; Agraït, N.; Vieira, S.; van Ruitenbeek, J. M. *Phys. Rev. B* **2002**, *66*, 085418.
(10) Shiota, T.; Mares, A. I.; Valkering, A. M. C.; Oosterkamp, T. H.; van Ruitenbeek, J. M. *Phys. Rev. B* **2008**, *77*, 125411.
(11) Bahn, S. R.; Jacobsen, K. W. *Phys. Rev. Lett.* **2001**, *87*, 266101.
(12) Rubio-Bollinger, G.; Bahn, S. R.; Agraït, N.; Jacobsen, K. W.; Vieira, S. *Phys. Rev. Lett.* **2001**, *87*, 026101.
(13) Stepanyuk, V. S.; Klavsyuk, A. L.; Hergert, W.; Saletsky, A. M.; Bruno, P.; Mertig, I. *Phys. Rev. B* **2004**, *70*, 195420.
(14) Fernández-Rossier, J.; Jacob, D.; Untiedt, C.; Palacios, J. J. *Phys. Rev. B* **2005**, *72*, 224418.
(15) da Silva, E. Z.; da Silva, A. J. R.; Fazzio, A. *Phys. Rev. Lett.* **2001**, *87*, 256102.

(16) Ribeiro, F. J.; Cohen, M. L. *Phys. Rev. B* **2003**, *68*, 035423.
(17) Kondo, Y.; Takayanagi, K. *Science* **2000**, *289*, 606.
(18) Tosatti, E.; Prestipino, S.; Kostlmeier, S.; Dal Corso, A.; Di Tolla, F. D. *Science* **2001**, *291*, 288.
(19) Delin, A.; Tosatti, E. *Phys. Rev. B* **2003**, *68*, 144434.
(20) Tung, J. C.; Guo, G. Y. *Phys. Rev. B* **2007**, *76*, 094413.
(21) Mokrousov, Y.; Bihlmayer, G.; Heinze, S.; Blügel, S. *Phys. Rev. Lett.* **2006**, *96*, 147201.
(22) Mokrousov, Y.; Bihlmayer, G.; Blügel, S. *Phys. Rev. B* **2005**, *72*, 045402.
(23) http://www.flapw.de.
(24) Li, C.; Freeman, A. J.; Jansen, H. J. F.; Fu, C. L. *Phys. Rev. B* **1990**, *49*, 5433.
(25) We calculate $\Delta E_{surf}$ by subtracting the surface energy of the corresponding element from ref 38 from the calculated energy difference $\Delta E_{bulk}$ between an atom in the bulk and an atom in a MW at $d_0$ (Figure 4a).
(26) In order to relate $E_{bulk}$ to the binding energy of the MW, we calculated the MWs in a 3D supercell at $d_0$. Supercell and bulk calculations have been performed with the same symmetry group. The same computational parameters were used for MW calculations with the 1D or bulk code.
(27) Untiedt, C.; Caturla, M. J.; Calvo, M. R.; Palacios, J. J.; Segers, R. C.; van Ruitenbeek, J. M. *Phys. Rev. Lett.* **2007**, *98*, 206801.
(28) Rego, L. G. C.; Rocha, A. R.; Rodrigues, V.; Ugarte, D. *Phys. Rev. B* **2003**, *67*, 045412.
(29) Cheng, D.; Kim, W. Y.; Min, S. K.; Nautiyal, T.; Kim, K. S. *Phys. Rev. Lett.* **2006**, *96*, 096104.
(30) Legoas, S. B.; Galvão, D. S.; Rodrigues, V.; Ugarte, D. *Phys. Rev. Lett.* **2002**, *88*, 076105.
(31) Smogunov, A.; Dal Corso, A.; Delin, A.; Weht, R.; Tosatti, E. *Nat. Nanotechnol.* **2008**, *3*, 22.
(32) The best description would probably be a combination of LDA and GGA, as for surface and bulk properties of 4d and 5d TMs an LDA description could be more appropriate, while GGA is better suited for chain properties. However, this makes a consistent comparison of chain and bulk total energies difficult.
(33) Häkkinen, H.; Moseler, M.; Landman, U. *Phys. Rev. Lett.* **2002**, *89*, 033401.
(34) Frederiksen, T.; Paulsson, M.; Brandbyge, M.; Jauho, A.-P. *Phys. Rev. B* **2007**, *75*, 205413.
(35) De Maria, L.; Springborg, M. *Chem. Phys. Lett.* **2000**, *323*, 293.
(36) Sánchez-Portal, D.; Artacho, E.; Junquera, J.; Ordejón, P.; García, A.; Soler, J. M. *Phys. Rev. Lett.* **1999**, *83*, 3884.
(37) Fernández-Seivane, L.; García-Suárez, V. M.; Ferrer, J. *Phys. Rev. B* **2007**, *75*, 075415.
(38) Skriver, H. L.; Rosengaard, N. M. *Phys. Rev. B* **1992**, *46*, 7157.

NL0800671